Antimicrobial Efficacy and Safety of a Novel Gas Plasma-Activated Catheter Lock Solution

Sudhir Bhatt,a Poonam Mehta,a Chen Chen,b Dayle A. Daines,c Leonard A. Mermel,d,e Hai-Lan Chen,a Michael G. Konga,f

aCenter for Bioelectrics, Old Dominion University, Norfolk, Virginia, USA

bState Key Laboratory of Electrical Insulation and Power Equipment, Center for Plasma Biomedicine, Xi'an Jiaotong University, Xi'an, Shaanxi, China

cDepartment of Biological Sciences, Old Dominion University, Norfolk, Virginia, USA

dDepartment of Medicine, Warren Alpert Medical School of Brown University, Providence, Rhode Island, USA

eDivision of Infectious Diseases, Rhode Island Hospital, Providence, Rhode Island, USA

fDepartment of Electrical and Computer Engineering, Norfolk, Virginia, USA

ABSTRACT Antimicrobial lock solutions are important for prevention of microbial colonization and infection of long-term central venous catheters. We investigated the efficacy and safety of a novel antibiotic-free lock solution formed from gas plasma-activated disinfectant (PAD). Using a luminal biofilm model, viable cells of methicillin-resistant *Staphylococcus aureus*, *Staphylococcus epidermidis*, *Pseudomonas aeruginosa*, and *Candida albicans* in mature biofilms were reduced by 6 to 8 orders of magnitude with a PAD lock for 60 min. Subsequent 24-h incubation of PAD-treated samples resulted in no detectable regrowth of viable bacteria or fungi. As a comparison, the use of a minocycline-EDTA-ethanol lock solution for 60 min led to regrowth of bacteria and fungi, up to 10^7 to 10^9 CFU/ml, in 24 h. The PAD lock solution had minimal impact on human umbilical vein endothelial cell viability, whereas the minocycline-EDTA-ethanol solution elicited cell death in nearly half of human endothelial cells. Additionally, PAD treatment caused little topological change to catheter materials. In conclusion, PAD represents a novel antibiotic-free, noncytotoxic lock solution that elicits rapid and broad-spectrum eradication of biofilm-laden microbes and shows promise for the prevention and treatment of intravascular catheter infections.

KEYWORDS gas plasma-activated disinfectant, catheter, lock solution, central venous catheter, central line-associated bloodstream infection

Central venous catheters (CVCs) provide long-term access to medication and total parenteral nutrition for cancer, hemodialysis, short-gut, and transplant patients. The majority of bloodstream infections in long-term CVCs ($>$10 days) are associated with intraluminal microbial colonization (1, 2). Current management guidelines for catheter-related bloodstream infections (CRBSIs) recommend use of antimicrobial lock therapy (ALT) for catheter salvage (3). Even with antibiotics at concentrations 1,000-fold above the systemic therapeutic dose, current ALT may be ineffective in eradicating mature bacterial and fungal biofilms (4–7). In addition, leakage of antimicrobial lock solutions into the bloodstream has been implicated in systemic toxicity in patients with long-term CVCs, potential for increased biofilm formation, and adverse effects on catheter integrity and intraluminal precipitation (5, 6, 8, 9).

After 3 decades of optimizing their utility in catheter lock solutions, reliance on current antibiotics is fundamentally challenged by the limited scope to improve the trade-off between efficacy and toxicity (6, 7, 10) and by the potential risk of antimicrobial resistance (11). This has motivated a considerable number of studies of antimi-

Address correspondence to Hai-Lan Chen, h1chen@odu.edu, or Michael G. Kong, mkong@odu.edu.
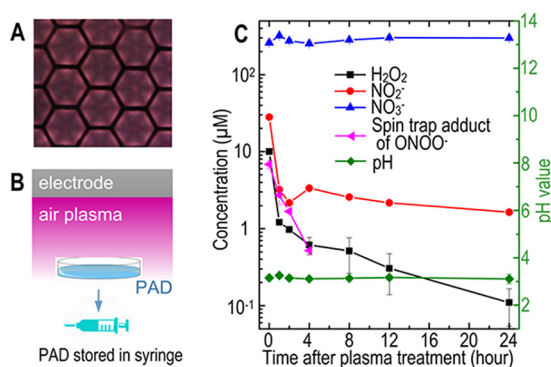
FIG 1 (A) End view of an atmospheric air plasma generated on the surface of its hexagon-shaped mesh electrode on a glass slide (in black), with each hexagon metal rim confining one surface discharge plasma (in purple). The air plasma was sustained at a peak-to-peak voltage of 9.4 kV at 23 kHz and a dissipated power density of 3.2 W. (B) A side view schematic of the surface plasma being used to treat 5 ml normal saline in a petri dish downstream from the electrode for 2 min. The resulting PAD was then stored in a sterile syringe. (C) Concentrations of H_2O_2, NO_2^-, NO_3^-, and spin-trap adducts of $ONOO^-$ as well as a pH of PAD at 37°C as a function of time after plasma activation of saline.

crobial properties of low-temperature gas plasma over the past 20 years (12–14). Known as the 4th state of matter after solid, liquid, and gas, gas plasma is formed by supplying a gas with sufficient energy (e.g., a high-voltage pulse) for its ionization (13). Gas plasma contains diverse reactive oxygen species and reactive nitrogen species (ROS and RNS, or RONS) as well as other effectors (e.g., transient charges), all changing dynamically (12–15). Antimicrobial properties of gas plasma and also gas plasma-activated liquid have been established extensively against bacteria, fungi, and viruses (12–14, 16, 17), and the modes of their actions include membrane and lipid peroxidation, protein oxidation, and DNA damage (12–17). It has been shown that RONS from gas plasma can be designed to be selective against microbes with little harm to the mammalian host (18, 19). The use of gas plasma for disinfection is inspired by the use of endogenous ROS by immune cells of a mammalian host to inactivate invading bacteria (12, 13).

As gas plasma endows its antimicrobial properties to its treated water (20), we developed a saline-based gas plasma-activated disinfectant (PAD) as a novel catheter lock solution. The aim of the current study was to determine the efficacy of PAD against bacteria and fungi in a catheter biofilm model and to assess the effect of PAD on primary human umbilical vein endothelial cells (HUVECs) as an *in vitro* model of blood vessel endothelium. In doing so, we used the PAD as a novel antibiotic-antiseptic lock solution.

RESULTS

Transient reactive oxygen and nitrogen species. Diverse reactive oxygen and nitrogen species in PAD were observed, with all long-lived RONS at a low concentration, with peak values at 10 to 300 μM (Fig. 1). The peak concentration of a given reactive species in PAD was markedly below the MIC of the species when acting alone. For example, the MICs of H_2O_2 and $ONOO^-$ are both 1 to 10 mM for *E. coli* (21, 22), and these are approximately 3 orders of magnitude above the peak concentrations of H_2O_2 (10 μM) and spin-trap adducts of $ONOO^-$ (7 μM) found in PAD (Fig. 1). Figure 1 shows half-lives of 30 to 45 min for H_2O_2, NO_2^-, and $ONOO^-$, as well as plasma-induced acidification (pH 3), with which the main reactive chlorine species was hypochlorous acid (HOCl) below 100 nM in air plasma-activated saline of greater than 1 mm in thickness (23), 3 orders of magnitude below its MIC of approximately 12.5 μM against *Staphylococcus aureus* (24). Peak concentrations of NO_2^- (30 μM) and NO_3^- (300 μM) were much lower than their MICs (>0.5 mM for NO_2^- and >10 mM for NO_3^-) (25) and cytotoxicity dose (>18 mM for NO_3^-) (26). Together, antimicrobial reactive species in PAD were at least 3 orders of magnitude below their individual MICs and were

TABLE 1 Survivors and regrowth of ATCC-derived isolates following PAD treatment[a]

Lock solution	Lock time (min)	Survivor population (log$_{10}$ CFU/ml ± SD)			Regrowth population (log$_{10}$ CFU/ml ± SD)		
		MRSA BAA-1707	P. aeruginosa BAA-47	C. albicans 14053	MRSA BAA-1707	P. aeruginosa BAA-47	C. albicans 14053
Untreated	0	7.97 ± 0.04	7.95 ± 0.03	6.92 ± 0.23	8.71 ± 0.09	9.05 ± 0.02	8.24 ± 0.09
Saline	60	7.58 ± 0.07	7.70 ± 0.07	6.56 ± 0.09	7.33 ± 0.08	7.95 ± 0.04	7.97 ± 0.07
M-EDTA-25E	15	5.30 ± 0.01	5.44 ± 0.04	4.80 ± 0.36	5.62 ± 0.05	6.24 ± 0.15	7.44 ± 0.13
	30	3.46 ± 0.10	2.97 ± 0.17	4.08 ± 0.18	5.48 ± 0.02	6.14 ± 0.14	6.66 ± 0.28
	45	<1	1.76 ± 0.44	3.87 ± 0.15	<1	6.18 ± 0.10	4.88 ± 0.03
	60	<1	<1	3.47 ± 0.23	<1	4.39 ± 0.02	4.43 ± 0.04
PAD	15	4.91 ± 0.11	3.92 ± 0.43	4.90 ± 0.35	3.13 ± 0.10	6.40 ± 0.07	6.76 ± 0.05
	30	<1	<1	3.21 ± 0.26	<1	6.27 ± 0.22	3.69 ± 0.09
	45	<1	<1	<1	<1	<1	1.91 ± 0.16
	60	<1	<1	<1	<1	<1	<1

[a]For all strains, $P \leq 0.001$ compared with the control ($n = 3$); detection limit, 1 log$_{10}$ CFU/ml.

transient, with H_2O_2, NO_2^-, and $ONOO^-$ half-lives of 30 to 45 min. Fundamentally distinct from antibiotics, PAD is characterized by chemical diversity of many RONS, each at low concentrations and decaying rapidly within 1 h.

Antimicrobial and antibiofilm efficacy. From an initial microbial load of 10^7 to 10^8 CFU/ml, the PAD lock eradicated 24-h luminal biofilms of methicillin-resistant *S. aureus* (MRSA) (BAA-1707) and *Pseudomonas aeruginosa* (BAA-47) within 30 min and *Candida albicans* 14053 within 45 min (Table 1). Complete suppression of regrowth in the segment lumens was confirmed at 24 h after an extended lock of 45 min for bacteria and 60 min for *C. albicans* (Table 1). However, the treatment with M-EDTA-25E (3 mg/ml minocycline hydrochloride and 30 mg/ml EDTA mixed in 25% ethanol) left a residual bacterial population of 3.0 to 3.5 log$_{10}$ CFU/ml with a 30-min incubation and a residual fungal population of 3.5 log$_{10}$ CFU/ml with a 60-min incubation (Table 1). Furthermore, 24-h incubation of segment lumens treated with M-EDTA-25E lock solution for 60 min led to recovery of *P. aeruginosa* and *C. albicans*, both to approximately 4.4 log$_{10}$ CFU/ml (Table 1). Against clinical isolates, PAD lock for 60 min led to a 6- to 8-log reduction of all bacterial and fungal test microorganisms (Table 2) and complete suppression of regrowth (Table 2). The same 60-min exposure to M-EDTA-25E lock solution resulted in approximately 2.8 log$_{10}$ CFU/ml of MRSA and *Staphylococcus epidermidis* and 4.3 log$_{10}$ CFU/ml of *C. albicans* in segment lumens (Table 2). Microbial recovery with M-EDTA-25E reached the initial luminal inoculum of 7 to 9 log$_{10}$ CFU/ml (Table 2).

A detailed comparison between PAD and M-EDTA-25E was made for eradication and regrowth of *C. albicans* 14053, with extended lock times of up to 360 min. Complete regrowth inhibition of *C. albicans* biofilm required 360 min with M-EDTA-25E, while a lock time of 60 min was needed for PAD (Table 3). Efficacy with 60-min PAD lock solution was confirmed against 48-h biofilms tested against microbes listed in Table 1 (data not shown).

To confirm effective biofilm dispersal, Fig. 2A shows that 60-min exposure to PAD removed adhesive materials from inoculated glass slides with MRSA BAA-1707 and *C. albicans* 14053. In contrast, M-EDTA-25E exposure for 60 min led to considerable

TABLE 2 Survivors and regrowth of clinical isolates following PAD treatment[a]

Lock Solution	Lock time (min)	Survivor population (log$_{10}$ CFU/ml ± SD)			Regrowth population (log$_{10}$ CFU/ml ± SD)		
		MRSA SO385	S. epidermidis M0881	C. albicans P57072	MRSA SO385	S. epidermidis M0881	C. albicans P57072
Untreated	0	8.51 ± 0.17	7.37 ± 0.13	6.64 ± 0.22	9.35 ± 0.07	9.40 ± 0.13	7.45 ± 0.16
Saline	60	6.66 ± 0.07	5.10 ± 0.16	5.62 ± 0.12	9.10 ± 0.22	8.82 ± 0.27	7.42 ± 0.12
M-EDTA-25E	30	5.59 ± 0.19	3.61 ± 0.12	4.93 ± 0.13	8.93 ± 0.10	9.03 ± 0.15	7.25 ± 0.17
	60	2.93 ± 0.20	2.84 ± 0.27	4.34 ± 0.34	8.83 ± 0.14	8.53 ± 0.08	7.21 ± 0.22
PAD	30	2.67 ± 0.16	2.47 ± 0.25	3.01 ± 0.33	8.94 ± 0.16	7.84 ± 0.26	6.55 ± 0.24
	60	<1	<1	<1	<1	<1	<1

[a]For all strains, $P \leq 0.05$ compared with the control ($n = 3$); detection limit, 1 log$_{10}$ CFU/ml.

TABLE 3 PAD and M-EDTA-25E efficacy at different lock dwell times against *C. albicans*

| Lock time (min) | *C. albicans* 14053 population[a] (log$_{10}$ CFU/ml ± SD) | | | |
| | M-EDTA-25E | | PAD | |
	Survivors	Regrowth	Survivors	Regrowth
0	7.25 ± 0.23	8.13 ± 0.27	7.25 ± 0.23	8.13 ± 0.27
30	5.89 ± 0.25	8.03 ± 0.22	5.25 ± 0.13	6.87 ± 0.19
60	4.87 ± 0.11	6.60 ± 0.17	<1	<1
120	4.34 ± 0.13	6.20 ± 0.32	<1	<1
180	2.60 ± 0.28	5.90 ± 0.30	<1	<1
240	<1	4.30 ± 0.27	<1	<1
300	<1	2.99 ± 0.25	<1	<1
360	<1	<1	<1	<1

[a]For all conditions, $P \leq 0.001$ compared with the control ($n = 3$); detection limit, 1 log$_{10}$ CFU/ml.

biomass remaining on glass slides (Fig. 2A). To confirm biofilm dispersal from catheter lumens, adhesive materials stained with crystal violet and dissolved from test lumens with ethanol were quantified with optical absorption at 590 nm. Results are shown in Fig. 2B and suggest that PAD exposure for 60 min reduced the optical absorption to approximately 1% compared to approximately 41% achieved with M-EDTA-25E.

Cytotoxicity to primary human cells. Figure 3 shows that a simulated spill of PAD minimally affected the viability of HUVECs at all evaluation points of 0.5, 2, 15, and 24 h. For the lock-to-medium ratio at both 0.1% and 0.5%, there was no statistically significant difference in the viability between treated and untreated HUVECs at 24 h, suggesting
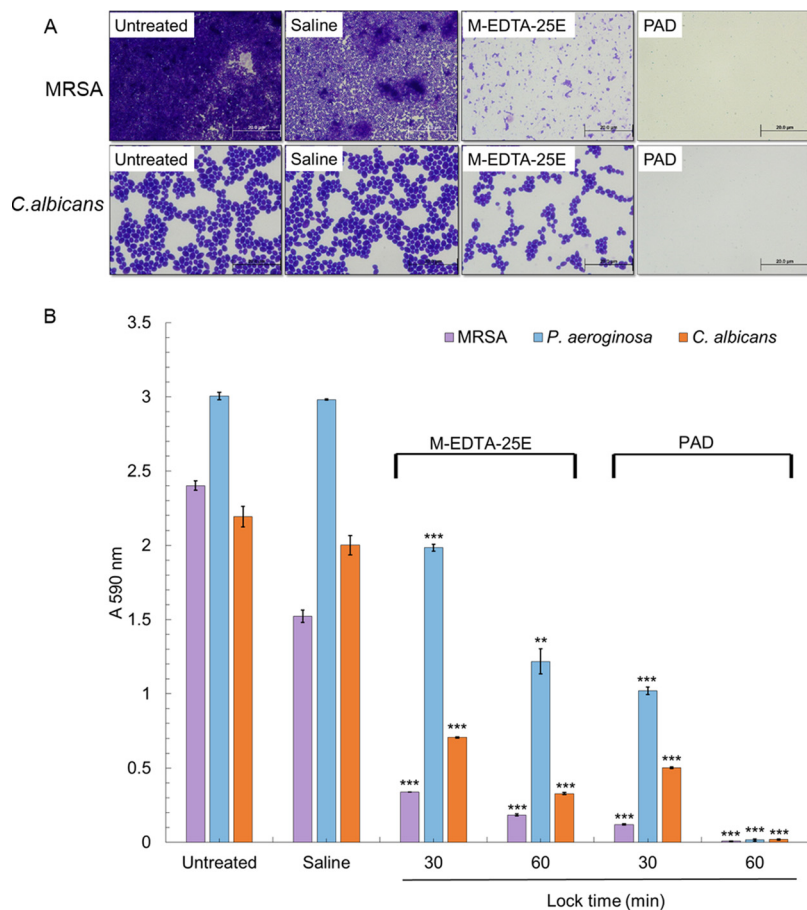

FIG 2 (A and B) Microscopic views of the biofilm formation in glass chambers after crystal violet (CV) staining (lens magnification, ×100) (A) and quantification of CV (B). $P \leq 0.005$ (***) and $P \leq 0.01$ (**) compared with the control. The scale bar is 20 μm.
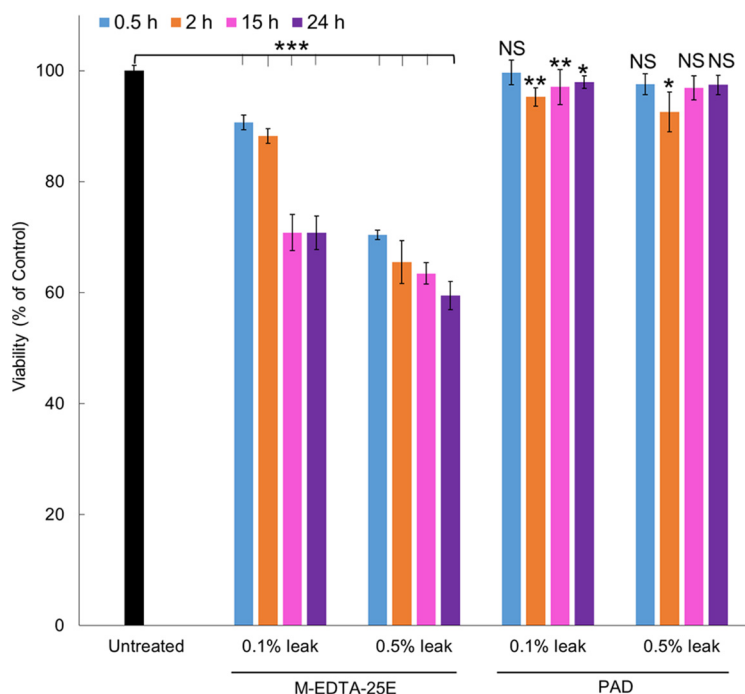
FIG 3 Evaluation of potential cytotoxic activity after exposure to HUVECs by leaked lock solution at solution-to-medium ratios of 0.1% and 0.5%. $n = 3$. $P \leq 0.01$ (**) and $P \leq 0.05$ (*) compared with the control. NS, not significant.

an effective repair of initial minor injuries in PAD-treated human cells. In contrast, the same amount of spilled M-EDTA-25E damaged HUVECs, with cell viability clearly lower at the lock-to-medium ratio of 0.5% than 0.1%. Viability of HUVECs treated with M-EDTA-25E became progressively decreased with incubation time, suggesting an accumulation of unrepaired injury. For the case of 24-h incubation when necessary repairs of cellular damage should have taken place, cell viability was 59% for M-EDTA-25E at the lock-to-medium ratio of 0.5%, suggesting cell death.

PAD effects on silicon catheter surface morphology. To test if the RONS in acidified PAD (Fig. 1) affects the catheter material after repeated PAD locking, we performed an accelerated aging test by continuously locking segments of catheter tubing for 7 days with regularly replenished PAD. In practice, PAD locking for 2 h per day is sufficient to ensure complete suppression of microbial regrowth (Tables 1 and 2). There was no evidence of any episodes of fissures, cracks, or other morphological abnormalities in PAD-treated catheter tubes (Fig. 4). When the test was repeated for polyurethane for 7 days, no evidence of any morphological abnormalities was found from scanning electron microscope (SEM) micrographs (data now shown).

DISCUSSION

Our study demonstrates that PAD lock solution is effective against microbial biofilms implicated in CRBSI with minimal cytotoxicity to primary human vein epithelial cells. Exposure to PAD lock for 60 min led to a reduction of viable bacterial and fungal biofilms of 6 to 8 orders of magnitude and completely suppressed their regrowth. Similarly, PAD lock exposure for 60 min substantially reduced all adherent matter on glass slides inoculated with MRSA or *C. albicans*. For *C. albicans* 14053, M-EDTA-25E required 6 h to achieve similar eradication and regrowth suppression. This is broadly in line with the capability of current ALT that generally requires prolonged lock times (27, 28).

Variable efficacy has been reported for current ALT and antifungal lock therapy (A*f*LT) (27, 28). For PAD therapy, effective lock times were approximately 60 min against the Gram-positive and Gram-negative bacteria as well as *C. albicans*, which we studied (Tables 1 and 2 and Fig. 2). This suggests that PAD therapy can be applied prior to
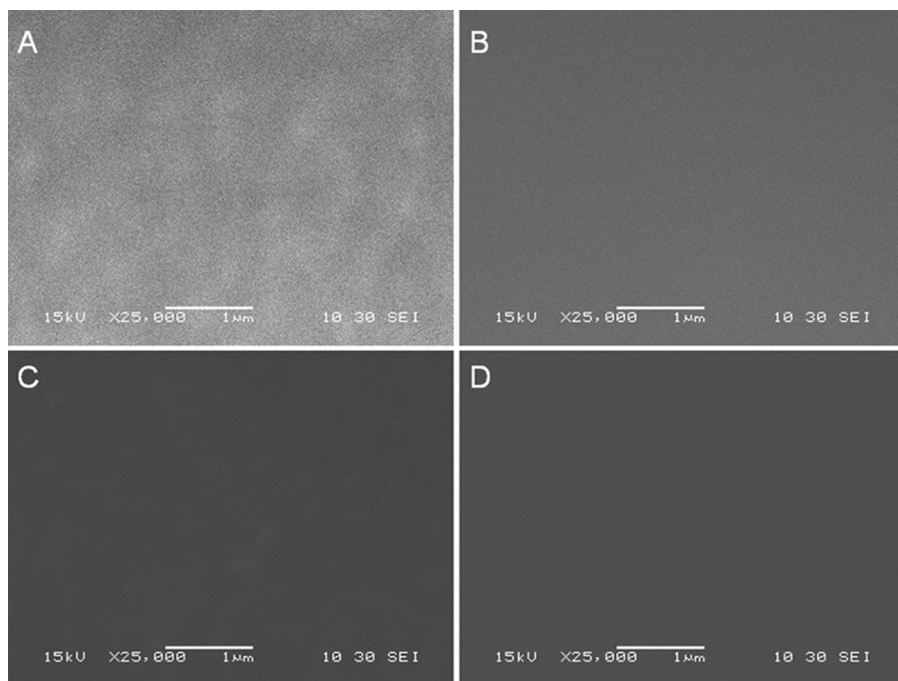
FIG 4 SEM micrographs (×25,000 magnification) of the luminal surface of silicone catheter tubing segments with the tubing segments as received from the manufactured (A), stored for 7 days at 37°C with no treatment (B), and treated with saline (C) or PAD (D) for 7 days at 37°C.

identification of pathogens that may be involved in a suspected CRBSI episode. The broad-spectrum antimicrobial properties of PAD are based on chemical diversity of reactive oxygen, nitrogen, and chlorine species (29) and collectively are capable of attacking different cellular targets (14, 15) with minimal risk of systemic toxicity (Fig. 3) or damage to silicone catheters (Fig. 4).

An additional advantage of PAD is that we found minimal toxicity upon exposure to primary human umbilical vein endothelial cells. This is likely benefited from pulsed RONS of PAD (Fig. 1), with which oxidative stresses to HUVECs are transient and as such are more easily repaired than chemicals that generate reactive oxygen species in living tissues for many months (39). Furthermore, continuous PAD locking for 7 days did not result in any morphological abnormalities of silicone, such as fissures, cracks, or damage when imaged using SEM (Fig. 4). The maximum daily exposure of a CVC to PAD is 2 h, and as such the impact of continuous PAD locking for 7 days would be equivalent to that of 2-h daily PAD therapy on an indwelling CVC for 84 hospital days [i.e., (7 × 24)/2]. PAD production and utility in the hospital setting is readily feasible with a table-top automated PAD-making machine having a footprint of 6 by 12 inches.

Potential limitations to this study are the limited number of microbes included and the facts that studies were not carried out in plasma or serum, only silicone material was tested, and additional testing was not performed to assess the impact of our PAD lock solution on the silicone tubes (e.g., testing the modulus of elasticity, force at break, and maximum stress at break).

PAD lock solution is free of antibiotics, and the mechanism of action does not involve specific binding sites on bacteria or fungi, thereby minimizing the risk of selecting for antimicrobial resistance (11). In this context, it is interesting that a 2-h exposure to a non-antibiotic-containing, nitroglycerin-based lock solution reduces bacterial and fungal intraluminal biofilms by 4 orders of magnitude (30, 31). Nitroglycerin produces reactive oxygen and nitrogen species (32), and this may explain why its activity against bacteria and fungi is of similarly broad spectrum to PAD. The high activity of PAD in both bacteria and fungi is associated, at least partly, with its chemical diversity (Fig. 1C) and their multiple cellular targets, including lipid peroxidation,

protein oxidation, and DNA damage (12–17). Recent evidence of DNA-protein cross-links in gas plasma-treated bacteria highlights the challenge for microbes to enable effective repair after plasma treatment (33). This lends further support to the superior activity of PAD. Taking these results together, PAD lock therapy may be an innovative addition to current ALT and AfLT.

MATERIALS AND METHODS

Catheter lock solutions. Minocycline hydrochloride (3 mg/ml) and EDTA (30 mg/ml) were mixed in 25% ethanol (M-EDTA-25E) as a comparator lock solution (34). PAD was formed by treating 5 ml of normal saline (NaCl) for 2 min with a room temperature gas plasma system at 3.2 W in ambient air (Fig. 1) (39). For results presented here, PAD usually was used within 5 min after its production. Untreated saline was used as a control.

Microorganisms and luminal biofilm model. MRSA BAA-1707, *P. aeruginosa* BAA-47, and *C. albicans* 14053 (ATCC, Manassas, VA) were used to test antimicrobial efficacy of PAD. Additionally, PAD was tested with clinical isolates of MRSA (SO385), *S. epidermidis* (M0881), and *C. albicans* (BEI, Manassas, VA), as well as a laboratory control strain of *P. aeruginosa* 27853 (ATCC, Manassas, VA). MRSA and *S. epidermidis* were grown on Luria-Bertani (LB) agar, *P. aeruginosa* on brain heart infusion (BHI) agar, and *C. albicans* on yeast-malt (YM) agar. A single colony was inoculated into 10 ml of appropriate broth, incubated overnight at 37°C with shaking at 160 rpm, harvested at mid-logarithmic phase by centrifugation (500 × g, 5 min), and then washed twice with 1× phosphate-buffered saline (PBS). The inoculum concentration was adjusted to 1.0×10^7 to 2.0×10^7 CFU/ml by broth dilution.

We modified a luminal biofilm model (4, 30) using sterile silicone tubing with an inner diameter of 1.58 mm and outer diameter of 3.175 mm (NewAge, Southampton, PA). Silicone tubing segments, 305 mm in length, were sterilized and inoculated with approximately 600 μl of a prepared microbial culture using a sterile syringe. Each inoculated catheter was sealed with a sterile, tight-fitting polytetrafluoroethylene plug, placed in a sterile petri dish, and incubated without shaking for 24 or 48 h at 37°C. Inoculated segments were gently flushed with normal saline, removing nonadherent microorganisms and leaving intact biofilm.

Eradication and regrowth assays. In the eradication assay, 600 μl of a test lock solution was slowly injected into the lumen of each inoculated segment using a syringe. Segments were then incubated at 37°C for 15 to 360 min. After incubation, the external surface of each segment was thoroughly swabbed with 70% (vol/vol) ethanol and allowed to air dry to ensure that only luminal microbes were recovered. Luminal contents were removed with a gentle saline flush, and each segment was then cut into three segments of 101.6 mm and submerged in 2 ml of 0.1 M glycine buffer (pH 7.0). Each of these segments was then vortexed for 1 min, sonicated at 40 kHz for 1 min in a room temperature water bath, and then vortexed for an additional minute. Luminal contents were then serially diluted and colony counts were enumerated using a plate counter (detection limit, 10 CFU/ml).

To evaluate microbial regrowth, catheter segments from each eradication treatment were placed in a sterile 15-ml Falcon tube filled with 2 ml of appropriate broth and incubated overnight with shaking at 37°C. Following incubation, segments were vortexed for 1 min and then sonicated for 1 min. A 200-μl aliquot of sonicated broth was used for serial dilution and plating. Plates were incubated overnight at 37°C before colony enumeration.

Luminal biofilm dispersal assay. Before and after PAD treatment, biofilms on the inner walls of catheter lumens were stained with 0.1% crystal violet (BD, Franklin Lakes, NJ) for 15 min at room temperature. Unbound dyes were washed away, and the lumens were left in the hood to air dry. The air-dried lumens were cut into three identical individual pieces and submerged in 2 ml of 95% molecular-grade ethanol for 30 min. Crystal violet dyes were dissolved in ethanol and quantitated by optical absorbance at 590 nm. Negative controls were uninfected catheter lumens. All experiments were performed in triplicate.

Slide biofilm dispersal assay. Glass chamber slides (Thermo Fisher Scientific, Fair Lawn, NJ) were inoculated with 500 μl of microbial cultures at 1.0×10^7 to 2.0×10^7 CFU/ml and then incubated for 24 h to form biofilm on the surface of the slides. To remove planktonic cells, the medium was aspirated off and the biomass washed three times with 1 ml of 1× PBS. Following gentle washing, biofilms were treated with 200 μl of lock solution for 60 min. Before and after exposure to the lock solution, various wells of the inoculated slides were stained with crystal violet (BD, Franklin Lakes, NJ) for imaging and quantification of any adherent material (35).

Cytotoxicity assay. To assess for cytotoxicity of inadvertently spilled test lock solutions, we used HUVECs (Lonza, Walkersville, MD) with the 3-(4,5-dimethylthiazol-2-yl)-2,5-diphenyltetrazolium bromide (MTT) assay using the Vybrant MTT cell proliferation assay kit (Invitrogen, CA, USA) according to the manufacturer's instructions. Briefly, HUVECs were seeded in endothelial basal medium (Lonza, Walkersville, MD) at 200 μl/well in 96-well plates at a density of 1.0×10^5 cells/ml 1 day prior to a cytotoxicity test. To determine the volume of test lock solution to treat HUVECs, we used the algorithm that the maximum lock solution escaping from a CVC is approximately 0.5 ml per event (36), and this solution is distributed in the amount of blood pumped in 1 to 2 heart beats (37), which is approximately 100 ml in a healthy adult. This corresponds to a lock solution/blood ratio of up to approximately 0.5% per spill. Given this, each test lock solution was mixed at 0.1 to 0.5% of the cell medium in each HUVEC-containing well of the 96-well plates. Untreated HUVECs served as controls. As it is very rare for current catheters to allow for more than one spill event during one heart beat (36, 37), the lock solution-to-blood ratio of

0.5% is likely to be the maximum even with multiple spills and represents the worst-case scenario. The total catheter solution in our study was 0.6 ml in volume.

Measurements of reactive species. Long-lived RONS in PAD at 37°C were measured with a microplate reader (FLUOStar, BMG Labtech, NC, USA) with the Amplex Red assay kit (Thermo Fisher Scientific, MA, USA) for H_2O_2 and the Griess reagent assay (Cayman Chemical Co., MI, USA) for nitrite (NO_2^-) and nitrate (NO_3^-). Similarly, short-lived RONS were measured at 37°C with an electron spin resonance (ESR) spectrometer (EMX+; Bruker, Germany) and spin traps (38). Specifically, DMPO (5,5-dimethyl-1-pyrroline N-oxide) was used for trapping hydroxyl radicals ($^\bullet OH$), and DTCS (diethyldithio-carbamate) and MGD (N-methyl-D-glucamine dithiocarbamate) were used for trapping nitric oxide ($NO^\bullet$) (all from Dojindo Laboratories, Kumamoto, Japan). Superoxide ($O_2^{\bullet-}$) and peroxynitrite ($ONOO^-$) were trapped using TEMPONE-H (1-hydroxy-2,2,6,6-tetramethyl-4-oxo-piperidine hydrochloride; from Enzo Biochem, USA). The ESR detection limit was approximately 100 nM.

Surface characterization. Surface topology of the inner wall of silicone catheter tubing was examined using a JSM-6060LV scanning electron microscope (SEM; JEOL, Japan). To mimic prolonged exposure, tubing segments were locked with 600 μl of PAD for 2 h at 37°C. Lock solutions then were replenished with 600 μl of freshly prepared PAD for another 2 h at 37°C. This was repeated 5 times consecutively in a day. After the last 2-h treatment, test segments were locked with freshly prepared PAD overnight (~14 h) at 37°C. The treatment procedure lasted 7 days. As controls, segments of silicone tubing were locked with normal saline with the same procedure as that for lock solution replacement and untreated segments were stored at 37°C, both for 7 days. Following the treatment, tubing segments were cut open, and the inner surface of each segment was gold-coated and examined with an SEM at a working voltage of 15 kV.

Statistical analysis. All test conditions were studied in at least three independent experiments. Data are presented as means $\pm$ standard deviations (SD). Student t test was used to determine significance between data points.

ACKNOWLEDGMENTS

REFERENCES

1. Raad I, Hachem R, Hanna H, Bahna P, Charzinikolaou Fang X, Jiang Y, Chemaly RF, Rolston K. 2007. Sources and outcome of bloodstream infections in cancer patients: the role of central venous catheters. Eur J Clin Microbiol Infect Dis 26:549–556. https://doi.org/10.1007/s10096-007-0320-6.

2. Worth LJ, Slavin MA. 2009. Bloodstream infections in haematology: risks and new challenges for prevention. Blood Rev 23:113–122. https://doi.org/10.1016/j.blre.2008.10.003.

3. Marschall J, Mermel LA, Fakih M, Hadaway L, Kallen A, O'Grady NP, Pettis AM, Rupp ME, Sandora T, Maragakis LL, Yokoe DS. 2014. Strategies to prevent central line-associated bloodstream infections in acute care hospitals. Infect Control Hosp Epidemiol 35:753–771. https://doi.org/10.1086/676533.

4. Shah CB, Mitttelman MW, Costerton JW, Parenteau S, Pelak M, Arsenault R, Mermel LA. 2002. Antimicrobial activity of a novel catheter lock solution. Antimicrob Agent Chemother 46:1674–1679. https://doi.org/10.1128/AAC.46.6.1674-1679.2002.

5. Ramos ER, Reitzel R, Jiang Y, Hachem RY, Chaftari AM, Chemaly RF, Hackett B, Pravinkumar SE, Nates J, Tarrand JJ, Raad II. 2011. Clinical effectiveness and risk of emerging resistance associated with prolonged use of antibiotic-impregnated catheters: more than 0.5 million catheter days and 7 years of clinical experience. Crit Care Med 39:245–251. https://doi.org/10.1097/CCM.0b013e3181feb83e.

6. Niyyar VD, Lok CE. 2013. Pros and cons of catheter-lock solutions. Curr Opin Nephrol Hypertens 22:669–674. https://doi.org/10.1097/MNH.0b013e328365ba53.

7. Zakhour R, Chaftari AM, Raad I. 2016. Catheter-related infections in patients with haematological malignancies: novel preventative and therapeutic strategies. Lancet Infect Dis 16:e241–e250. https://doi.org/10.1016/S1473-3099(16)30213-4.

8. Mermel LA, Alang N. 2014. Adverse effects associated with ethanol catheter lock solutions: a systematic review. J Antimicrob Chemother 69:2611–2619. https://doi.org/10.1093/jac/dku182.

9. Luther MK, Bilida S, Mermel LA, LaPlante KL. 2015. Ethanol and isopropyl alcohol exposure increases biofilm formation in Staphylococcus aureus and Staphylococcus epidermidis. Infect Dis Ther 4:219–226. https://doi.org/10.1007/s40121-015-0065-y.

10. Messing B, Peitra-Cohen S, Debure A, Beliah M, Bernier JJ. 1988. Antibiotic-lock technique: a new approach to optimal therapy for catheter-related sepsis in home-parenteral nutrition patients. J Parenter Enteral Nutr 12:185–189. https://doi.org/10.1177/0148607188012002185.

11. Spellberg B, Bartlett JG, Gilbert DN. 2013. The future of antibiotics and resistance. N Engl J Med 368:299–302. https://doi.org/10.1056/NEJMp1215093.

12. Kong MG, Kroesen G, Morfill G, Nosenko T, Shimizu T, van Dijk J, Zimmermann JL. 2009. Plasma medicine: an introductory review. New J Phys 11:115012. https://doi.org/10.1088/1367-2630/11/11/115012.

13. Laroussi M, Kong MG, Morfill G, Stolz W (ed). 2012. Plasma medicine: applications of low-temperature gas plasmas in medicine and biology. Cambridge University Press, Cambridge, United Kingdom.

14. Mai-Prochnow A, Murphy AB, McLean KM, Kong MG, Ostrikov K. 2014. Atmospheric pressure plasmas: infection control and bacterial responses. Int J Antimicrob Agents 43:508–517. https://doi.org/10.1016/j.ijantimicag.2014.01.025.

15. Vatansever F, de Melo WCMA, Avci P, Vecchio D, Sadasivam M, Gupta A, Chandran R, Karimi M, Parizotto NA, Yin R, Tegos GP, Hamblin MR. 2013. Antimicrobial strategies centered around reactive oxygen species–bactericidal antibiotics, photodynamic therapy, and beyond. FEMS Microbiol Rev 37:955–989. https://doi.org/10.1111/1574-6976.12026.

16. Joshi SG, Cooper M, Yost A, Paff M, Ercan U, Fridman G, Brooks AD. 2011. Nonthermal dielectric-barrier discharge plasma-induced inactivation involves oxidative DNA damage and membrane lipid peroxidation in Escherichia coli. Antimicrobial Agent Chemother 55:1053–1062. https://doi.org/10.1128/AAC.01002-10.

17. Kvam E, Davis B, Mondello F, Garner AL. 2012. Nonthermal atmospheric plasma rapidly disinfects multidrug-resistant microbes by inducing cell surface damage. Antimicrobial Agent Chemother 56:2028–2036. https://doi.org/10.1128/AAC.05642-11.

18. Isbary G, Heinlin J, Shimizu T, Zimmermann JL, Morfill G, Schmidt HU, Monetti R, Steffes B, Bunk W, Li Y, Klaempfl T, Karrer S, Landthaler M, Stolz W. 2012. Successful and safe use of 2 min cold atmospheric argon plasma in chronic wounds: results of a randomized controlled trial. Br J Dermatol 167:404–410. https://doi.org/10.1111/j.1365-2133.2012.10923.x.

19. Xu DH, Cui QJ, Xu YJ, Wang BC, Tian M, Li QS, Liu ZJ, Liu DX, Chen HL, Kong MG. 2018. Systemic study on the safety of immune-deficient nude

mice treated by atmospheric plasma-activated water. Plasma Sci Technol 20:044003. https://doi.org/10.1088/2058-6272/aa9842.

20. Kamgang-Youbi G, Herry JM, Bellon-Fontaine MN, Brisset JL, Doubla A, Naitali M. 2007. Evidence of temporal postdischarge decontamination of bacteria by gliding electric discharges: application to *Halnia alvei*. Appl Environment Microbiol 73:4791–4796. https://doi.org/10.1128/AEM.00120-07.

21. Imlay JA, Linn S. 1986. Bimodal pattern of killing of DNA-repair-defective or anoxically grown *Escherichia coli* by hydrogen peroxide. J Bacteriol 166:519–527. https://doi.org/10.1128/jb.166.2.519-527.1986.

22. Lindemann C, Lupilova N, Muller A, Warscheid B, Meyer HE, Kuhlmann K, Eisenacher M, Leichert LI. 2013. Redox proteomics uncovers peroxynitrite-sensitive proteins that help *Escherichia coli* to overcome nitrosative stress. J Biol Chem 288:19688–19714. https://doi.org/10.1074/jbc.M113.457556.

23. Liu ZC, Guo L, Liu DX, Rong MZ, Chen HL, Kong MG. 2017. Chemical kinetics and reactive species in normal saline activated by a surface air discharge. Plasma Process Polym 14:1600113. https://doi.org/10.1002/ppap.201600113.

24. Wang L, Bassiri M, Najafi R, Najafi K, Yang J, Khosrovi Hwong W, Barati E, Belisle B, Celeri C, Robson MC. 2007. Hypochlorous acid as a potential wound care agent. Part I. Stabilized hypochlorous acid: a component of the inorganic armamentarium of innate immunity. J Burns Wounds 6:65–79.

25. Xia DS, Liu Y, Zhang TCM, Yang SH, Wang SL. 2006. Antimicrobial effect of acidified nitrate and nitrite on six common oral pathogens *in vitro*. Chin Med J 119:1904–1909.

26. Clements WT, Lee S-R, Bloomer RJ. 2014. Nitrate ingestion: a review of the health and physical performances effects. Nutrients 6:5224–5264. https://doi.org/10.3390/nu6115224.

27. Vassallo M, Dunais B, Roger PM. 2015. Antimicrobial lock therapy in central-line associated bloodstream infections: a systemic review. Infection 43:389–398. https://doi.org/10.1007/s15010-015-0738-1.

28. Walraven CJ, Lee SA. 2013. Antifungal lock therapy. Antimicrob Agent Chemother 57:1–8. https://doi.org/10.1128/AAC.01351-12.

29. Carlsson S, Wiklund NP, Engstrand L, Weitzberg E, Lundberg JON. 2001. Effects of pH, nitric, and ascorbic acid on nonenzymatic nitric oxide generation and bacterial growth in urine. Nitric Oxide 5:580–586. https://doi.org/10.1006/niox.2001.0371.

30. Reitzel RA, Rosenblatt J, Hirsh-Ginsberg C, Murray K, Chaftari AM, Hachem R, Raad I. 2016. *In vitro* assessment of the antimicrobial efficacy of optimized nitroglycerin-citrate-ethanol as a nonantibiotic, antimicrobial catheter lock solution for prevention of central line-associated bloodstream infection. Antimicrob Agent Chemother 60:5175–5181. https://doi.org/10.1128/AAC.00254-16.

31. Chaftari AM, Hachem R, Szvalb A, Taremi M, Granwehr B, Viola GM, Sapna A, Assaf A, Numan Y, Shah P, Gasitashvilli K, Nativdad E, Jiang Y, Slack R, Reizel R, Rosenblatt J, Mouhayer E, Raad I. 2017. A novel nonantibiotic nitroglycerin-based catheter lock solution for prevention of intraluminal central venous catheter infections in cancer patients. Antimicrob Agent Chemother 61:e00091-17. https://doi.org/10.1128/AAC.00091-17.

32. Wenzel P, Mollnau H, Oelze M, Schulz E, Wickramanayake JMD, Muller J, Schuhmacher S, Hortmann M, Baldus S, Gori T, Brandes RP, Munzel T, Daiber A. 2008. First evidence for a crosstalk between mitochondrial and NADPH oxidase-derived reactive oxygen species in nitroglycerin-triggered vascular dysfunction. Antioxid Redox Signal 10:1435–1447. https://doi.org/10.1089/ars.2007.1969.

33. Guo L, Zhao YM, Liu DX, Liu ZC, Chen C, Xu RB, Tian M, Wang X, Chen H, Kong MG. 2018. Cold atmospheric-pressure plasma induces DNA-protein crosslinks through protein oxidation. Free Radic Res 28:1–16. https://doi.org/10.1080/10715762.2018.1471476.

34. Raad I, Henna H, Dvorak TM, Chaiban G, Hachem R. 2007. Optimal antimicrobial catheter lock solution, using different combinations of minocycline, EDTA, and 25-percent ethanol, rapidly eradicates organisms embedded in biofilms. Antimicrob Agent Chemother 51:78–83. https://doi.org/10.1128/AAC.00154-06.

35. O'Toole GA. 2011. Microtiter dish biofilm formation assay. J Vis Exp 30:2437.

36. Polaschegg HD, Shah C. 2003. Overspill of catheter lock solution: safety and efficacy aspects. ASAIO J 49:713–715. https://doi.org/10.1097/01.MAT.0000094040.54794.2D.

37. Polaschegg HD, Sodemann K. 2003. Risks related to catheter locking solutions containing concentrated citrate. Nephrol Dial Transplant 18:2688–2690.

38. Chen C, Li F, Chen HL, Kong MG. 2017. Aqueous reactive species induced by a PCB surface microdischarge air plasma device: a quantitative study. J Phys D App Phys 50:445208. https://doi.org/10.1088/1361-6463/aa8be9.

39. Hu J, Liu Y-F, Wu C-F, Xu F, Shen Z-X, Zhu Y-M, Li JM, Tang W, Zhao WL, Wu W, Sun HP, Chen QS, Chen B, Zhou GB, Zelent A, Waxman S, Wang ZY, Chen SJ, Chen Z. 2009. Long-term efficacy and safety of all-trans retinoic acid/arsenic trioxide-based therapy in newly diagnosed acute promyelocytic leukemia. Proc Natl Acad Sci U S A 106:3342–3347. https://doi.org/10.1073/pnas.0813280106.